Journal of Geology & Geophysics
ISSN: 2381-8719

Yang and Tang, J Geol Geophys 2017, 6:1
DOI: 10.4172/2381-8719.1000276

Research Article Open Access

Geochemistry Features of Oil-Gas Inclusions and UV-VIS Micro-spectra Analysis of Single Oil-Gas Inclusions in Bai 95 Oil Well

Yang AL[1]* and Tang MM[2]

[1]*Department of Physics, Ocean University of China, Qingdao, China*

[2]*China University of Petroleum (East China), Research Institute of Unconventional Oil & Gas and Renewable Energy, Qingdao, China*

Abstract

Geochemistry features including homogenization temperature (T_h), salinity (S), grains containing oil-gas inclusions (GOIs), and polarized fluorescence microscope identification of oil and gas inclusions (OGIs) of Bai 95 oil well (localized in Jilin Oil Field, Songliao Basin, Northeast China) were obtained. The oil and gas charging, maturities of palaeo-oils and gases, and the features of maternal source rocks related to three strata of Bai 95 oil well were estimated.

A low cost measurement system combing a common inverted fluorescence microscope (IMF) and an ultraviolet-visible (UV-VIS) spectrometer together was used to measure the micro-spectra of single OGIs. A minimum focus spot with 12 μm was obtained. The fluorescence interference from background was greatly decreased by subtracting the fluorescence from background. The micro-spectra from single OGIs take more information than that of traditional fluorescence spectra. The calculated Commission Internationale de l'Éclairage (CIE) chromaticity coordinates of the single OGIs by VIS spectra are more objective than judging colors of OGIs by human eyes. The main aromatic constitutes in the single OGIs were estimated by the UV-VIS spectra. With the buried depth increasing, the fluorescence peaks have red shifts; the aromatic hydrocarbons tend to become heavy. The UV-VIS spectra showed that there may be two maternal sources charging the strata in the second episode, one is mature, the other is low mature. This result coincides with the analysis result from geochemistry. Our experimental results showed this technique is a low cost, reliable and promising technique in measuring the UV-VIS fluorescence spectra of micro samples. The main aromatic hydrocarbons, the maturities of palaeo-oils and gases and the features of the maternal sources can be estimated by UV-VIS micro-spectroscopy of single OGIs.

Keywords: Geochemistry features; Single oil-gas inclusions; UV-VIS micro-spectra; Chromaticity analysis; Aromatic contents; Maturities of palaeo-oils and gases

Introduction

Micro-spectra are very important for OGIs because they take rich information about the palaeo-oils [1-5]. The properties of micro-fluorescence spectra of OGIs are largely controlled by the aromatic composites trapped in the OGIs. Generally, by analysis of the spectra, the main aromatic hydrocarbons, palaeo oil-gas maturity, and oil and gas charging history can be largely estimated [2,3,6-13]. And by the abundance of GOI [10,14], the petroleum characteristics of the corresponding stratum can be qualitatively determined.

According to the wavelength measurement range, micro fluorescence spectroscopy includes in VIS and UV-VIS spectra techniques. The VIS spectra technique includes fluorescence micro photometry (FMP), fluorescence alteration of multiple macerals (FAMM) and laser scanning confocal microscope (LSCM).

Burruss [15] described the analytical setup and method about FMP. Musgrave et al. [8] assumed separate lamp and scanning monochromator and photo multiplier tube (PMT) detector modules to obtain the luminescence and synchronously scanned luminescence spectra of single OGIs. The data collected from the technique are pertinent to evaluating systems and providing quantitative data for solving problems in oil migration and maturation determinations, oil-to-oil and oil-to-source correlations, oil degradation, and episodes and chemistry of cementation. Blanchet et al. [16] used a frequency doubler to obtain 360 nm pulse laser to excite single OGIs with size down to 1.7 μm. Alderton et al. [17] obtained the emission fluorescence spectra from individual inclusions in the range of 400-700 nm on a Zeiss UMSP 50 spectrometer with an HBO 100 Hg source, a 395 nm barrier filter and a variable aperture mask to isolate fluorescence from individual inclusions. Schubert et al. [18] acquired fluorescence spectra of the petroleum inclusions by a Leitz™MPVII spectrometer mounted on a Leitz microscope. Caja et al. [11,12] measured the fluorescence spectra of hydrocarbon inclusions by FMP. The results showed that Q580 index (580-700 nm vs. 400-580 nm areas) is very sensitive to the total composites of the petroleum. Bourdet et al. [19] measured the fluorescence spectra of petroleum inclusions over the range of 400-900 nm with an Avantes spectrometer equipped with a thermo-electric cooled Sony charge-coupled device (CCD) detector. The spectrometer was coupled to an Olympus AX70 microscope equipped with a 100 W high pressure mercury-vapor light source. FMP was also widely used to measure the vitrinite reflectivety of coal and source rock [20,21].

Because the fluorescence colors of OGIs are related to the chemical constitutes, the colors of OGIs are seen as indicators of maturities of palaeo-oils and gases [22]. But the colors of OGIs estimated by eyes are subjective and easily influenced by the observing environments [23]. For more precise determination of the colors of OGIs, more and more authors [14,16-19] calculated the CIE chromaticity coordinates according to the FMP spectra. McLimans's research results [6] showed

***Corresponding author:** Yang AL, Department of Physics, Ocean University of China, Qingdao, 266100, China, Tel: +8653266781208; E-mail: ailingy@ouc.edu.cn

Received November 23, 2016; **Accepted** December 05, 2016; **Published** December 09, 2016

Citation: Yang AL, Tang MM (2017) Geochemistry Features of Oil-Gas Inclusions and UV-VIS Micro-spectra Analysis of Single Oil-Gas Inclusions in Bai 95 Oil Well. J Geol Geophys 6: 276. doi: 10.4172/2381-8719.1000276

that as the oils increase in maturities, the x (red) and y (green) chromaticity coordinates decrease, i.e. the fluorescence emission moves towards the blue corner of the CIE diagram. Further examples of crude oils and OGIs have been analyzed using these diagrams. Blanchet et al. [16] gave a detailed analysis of OGIs from the North Sea and calibrated oils using CIE diagrams. They observed that the fluorescence colors of inclusion oils are variable even within a single fluid inclusion assemblage and they advanced a number of explanations for this based on geological processes. Bourdet et al. [14,19] expressed the variability in fluorescence colors from OGIs by CIE diagrams. Compared to subjective observation colors of oil inclusion, the CIE method provides more consistent results [5,6,16,18].

Except for calculating CIE chromaticity coordinates by VIS spectra of OGIs, the fluorescence spectra were also correlated with the American Petroleum Institute (API) degree of chemical constitutes and other geochemistry parameters of crude oils. Stasiuk and Snowdon [24] measured the micro-fluorescence spectra of artificially synthesized hydrocarbon inclusions and natural hydrocarbon inclusions. The migration of oil and gas was revealed. Chi et al. [25], Kirkwood et al. [9], Blanchet et al. [16], and Bourdet et al. [14,19] also used the fluorescence spectral data to estimate the API gravity of the entrapped fluids.

In 1992, Wilkins et al. [26] combined laser with microscope and established FAMM technique. Wilkins et al. [26,27] assumed FAMM technique to probe the relation between vitrinite inhibiting and fluorescence intensity changing with time. The result showed that FMMA can effectively correct inhibiting effect of vitrinite reflectivity before the stage of high maturity. Lo et al. [28] and Veld et al. [29] used this technique to measure the maturity of source rock. With the help of FMMA, Xiao et al. [30] used a laser induced fluorescence microscopy (LIFM) to study the carbonate rocks with higher maturities. For the emitting wavelengths of lasers cannot match well with the absorption bands of most materials and the low safe threshold (<5 μW) of lasers to human eyes, up to date, it is not a good choice to use lasers to excite the fluorescence of single OGI. With the progress of semiconductor lasers and solid-state lasers, low cost UV and violet (375 nm and 405 nm) lasers will be stable and reliable light sources, which will be integrated with CCD based spectrometers, so it is possible to develop and implement a standard OGI measurement and analysis methodology based on fluorescence spectroscopy [5].

LSCM is a very important technique for single OGIs. By LSCM, a point light source illuminating and a point image were realized. The images have higher space resolution and good quality. By controlling the movement of the objective, LSCM can realize continues optical section by tomography similar to computed tomography (CT) [3,31,32]. After computer imaging, a 3D profile of a micro sample could be recovered [33-35]. LSCM was used to obtain precise volume ratios between liquid phase and gas phase in OGIs [36-38]. Combining homogenization temperature, gas chromatography-mass spectrometer (GC-MS) analysis and PVTsim software, the pressure of palaeo-liquid can be obtained [37,39-44]. Furthermore, the depth of the stratum existing palaeo-liquid can also be obtained by the pressure. This is meaningful to study the migration of oil, gas and reservoir formation [42]. LSCM has special superiors as resolving the fluorescent macerals with micrometer sizes (source rock and oil shale). Stasiuk [45] used LSCM to observe algae in oil shale. Although LSCM has a higher space resolution and good image quality, till now the shortest laser wavelength of semiconductor laser is 370 nm, the fluorescence of single OGI obtained by LSCM is still in the range of VIS.

By above techniques, one can only obtain VIS spectra of OGIs. But some aromatic hydrocarbons in OGIs emit UV fluorescence which cannot be measured by above methods. Pironon and Pradier [46] investigated the UV fluorescence alteration of natural and synthetic hydrocarbon fluid inclusions. The results showed that the alteration of the inclusions fluorescence depends both on the nature of the oil and on the nature of the host crystal. There is no significant alteration for inclusions trapped in quartz crystals. Bourdet et al. [14] coupled an Ocean Optics USB2000-FL spectrometer to an Olympus AX 70 microscope with a 100 W high pressure mercury-vapor light source and measured fluorescence spectra of single oil inclusions with a bandwidth between 350 nm and 1000 nm. When using the Q ratio from Stasiuk and Snowdon [24] (Q Intensity 650 nm/Intensity 500 nm), the value visually blue fluorescing inclusions was often low or equal to 0. So Bourdet et al. [14] defined a new parameter called Green/Blue (QG/B) ratio (I510/I430). With their equipment a blue fluorescing oil inclusion has a QG/B value lower than 1, whereas a yellow fluorescing oil inclusion has a value higher than 1. Kihle [47] established a UV-VIS micro-spectra measurement system by combining an upright deep ultraviolet (DUV) microscope and a UV-VIS spectrometer together. The setup could be successfully used to measure the UV-VIS or VIS [48] spectra of single OGIs. But it is very expensive and users need to rebuild the microscope itself. Yang et al. [49] integrated a UV-VIS spectra measurement system by combining a common IFM, a reflective microscope objective (RMO), a UV-VIS spectrometer and a fiber cable together. For using the common IFM, the cost of the measurement system was greatly decreased. And the user needn't to rebuild the microscope. The system has the functions of micro-area location, external (from the spectrometer) or internal (from the microscope) light sources excitation, weak fluorescence detection and real-time taking photos. The UV-VIS spectra or VIS spectra of single OGIs were measured under excited by external light source [50,51].

In this paper, the geochemistry features OGIs from Bai 95 oil well (localized in Jilin Oil Field, Songliao Basin, Northeast China) including T_h, *S*, GOIs, and polarized fluorescence microscope identification were obtained. The previously established UV-VIS experiment system based on the IFM was used to measure the UV-VIS and VIS spectra of single OGIs of Bai 95 oil well. The CIE chromaticity coordinates of the OGIs was calculated by the VIS spectra. The main aromatic hydrocarbons were estimated by the UV-VIS spectra of single OGIs. Combining T_h, *S*, abundance of GOIs and polarized fluorescence microscope identification of OGIs, the episodes, maturity of palaeo-oil, and oil-gas charging were estimated.

Geological Setting

Songliao Basin is a large and fault-depression superimposed basin with two sets of hydrocarbon combinations developed in shallow-middle layer and deep layer. The Jilin Oil Field localizes in Songliao Basin, Northeast China (Figure 1). Many authors investigated the geological features and oil-gas reservoirs [52,53] of Songliao Basin, especially for southern area [54-58]. Few authors [59-61] studied the west slope of southern area of Songliao Basin. The under studied oil well of Bai 95 is in the west slope of southern area. Figure 1 shows the location of Bai 95 oil well and the interpolated thickness distribution of second member of Nenjiang Formation (K_2n_2) in Jilin Oil Field. The core of Bai 95 oil well is related to four members. K_2n_2 Member (382-395 m) mainly developed tender gray, grayish green mudstone and sandstone with parallel bedding. Finer facies were interpreted as pro-delta deposits. Yao Formation (412-437 m) is divided into two Members: K_2y_1 Member (423-437 m) and K_2y_{2+3} Member (412-423 m). Core observation indicates that K_2y_1 mainly developed gray, grayish

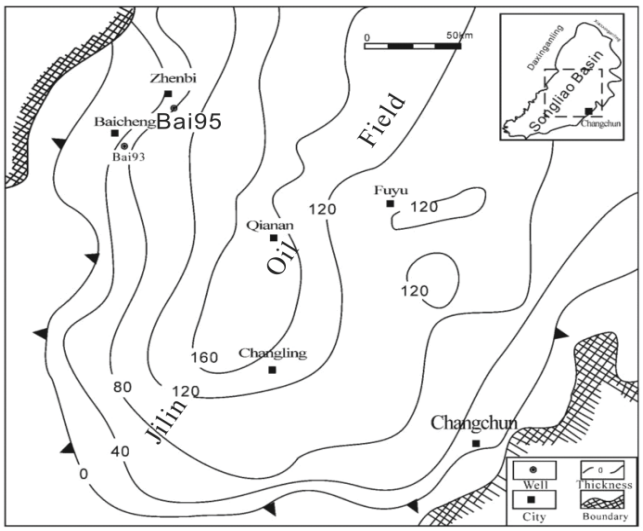

Figure 1: Location of sampling oil well of Bai 95 and interpolated thickness distribution of K_2n_2 Formation in Jilin Oil Field, Northeast China. The inset is the location of Jilin Oil Field in Songliao Basin.

green sandstone, and a small amount of silt mudstone. K_2y_{2+3} member mainly developed sandstone with flow ripples and low angle cross bedding structures. Oil immersion and oil spots are common in Yao Formation. The second member of Qingshankou Formation (K_2q_{n2}) mainly developed deep dark, gray mud stone and silt stone with parallel bedding and some very small scale ripple cross lamina. All sediment structures indicate braided delta plain deposits and shallow water environment. The under studied sandstone samples were taken from three depths: (1) K_2y_{2+3}, 419.3 m and 420.1 m; (2) K_2y_1, 435.0 m and (3) K_2q_{n2}, 494.6 m.

Experimental Setup

By the fluorescence color of OGI one can guess the maturity of palaeo oil and gas trapped in the mineral grains. But the fluorescence colors judged by human eyes are subjective. The observation result will be easily influenced by concrete observer and experimental environment. The wavelength range is limited (400-780 nm). In fact, the observation color of the OGI is often collect result, which includes not only the fluorescence from the under studied OGI, but also fluorescence from other OGIs trapped in the same grain, the cement around the mineral grain and even the mineral grain itself. The other OGIs may not be the same generation as the under studied OGI. What' more, the fluorescence intensity of the cement may stronger than that of the under studied OGI. So the fluorescence from the under studied OGI often add together with the fluorescence from the background. This makes the OGI looks like immersed into a colorful fluorescence cloud under microscope. And the judgment based on the fluorescence color of OGI will lead to a decreasing reliability. Thus it is necessary to establish an experimental setup to measure the fluorescence of single OGI. Because some aromatic hydrocarbons emit fluorescence in UV region, so the fluorescence spectra of the OGIs should be extended to UV-VIS range. And the excited light source should be a DUV light.

Figure 2 shows the schematic diagram of the experimental setup [49-51]. It includes seven parts: an IFM (1), a RMO (2), a fiber cable (3), a micro lens (4), a 3D adaptor (5), a UV-VIS spectrometer (6) and a computer (7). The IFM includes an internal light source (mercury arc lamp), three (violet, blue and green) band pass filters and fluorescence "cubes". Via the three band pass filters, the central wavelengths of violet, blue and green lights are at 365, 465, and 546 nm respectively. And the corresponding full width at half maximum (FWHM) are 12, 45 and 5 nm respectively. There are five differences between this system and Kihle's setup [47]. (1) A common and cheap IFM was used but not an expensive upright DUV microscope. The 3D adjustable adaptor can be conveniently connected to the main body of the IFM and one does not need any rebuilding to the microscope. (2) It is easy to adjust the RMO and the IMF coaxial. When the switch of the light source of IMF is on and the intensity of the light source is in minimum, one can adjust the 3D adjustable adaptor while observing the reflected light intensity from the RMO. When the intensity of the reflective beam is maximal, the two are coaxial. (3) The RMO has many advantages over a refractive objective. It is an all-reflective construction and free from chromatic aberration and astigmatism. The primary spherical aberration, primary coma and primary astigmatism have been corrected. The specific mirror coating of the RMO is the UV-enhanced aluminium film, which has as high as 89% average reflectivity in the range of 190 nm-10 m and is highly recommended for most DUV and UV use. Compared with the refractive objective, the RMO has stronger focusing ability. (4) The RMO has a relative large numerical aperture (0.65), so it can be used as an excellent focusing element and also a good component to effectively collect fluorescence; (5) One can use the video head settled on the microscope itself to take photos for the sample and the focusing spot in time.

In the setup, the spectrometer is a type of Floramax-4 (Horiba Jobin Yvon) with a 150 W xeon lamp (as external light source, 190-1100 nm) and a single photon PMT. The RMO was made of Ealing (52X). The micro-lens and the fiber cable were bought from Avantes Company. The diameter of the fiber is 400 μm and has a 90% transmittance in the range of 240-800 nm. There are seven fibers in the fiber cable. The fibers were arranged like a club. The middle one was as excitation fiber to guide the monochromatic excitation light from the external light source in the spectrometer to the micro-lens. After focused by the micro-lens and the RMO, a small light spot with size about 12-20 μm could be obtained and incidents on the studied OGI. The peripheral six fibers were as emission fibers to guide the fluorescence from single OGI into the detector in the spectrometer for spectra measurement. For prevent the scattering light coming from single OGI or background arriving at the detector, a 280 nm or 380 nm barrier filters was respectively put in the front of the emission window of the spectrometer when external light source was used as excitation light (250 nm and 365 nm). The two

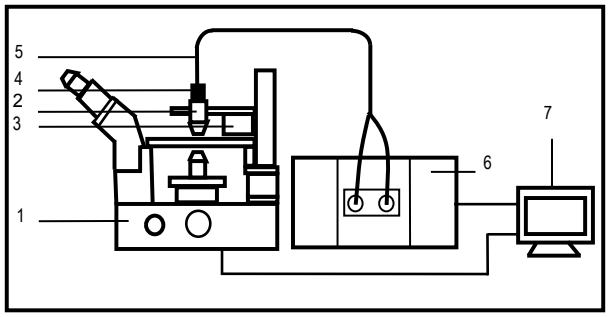

Figure 2: Schematic diagram of the micro-spectroscopy setup based on a common inverted fluorescence microscope. In which, 1-inverted fluorescence microscope (IMF); 2-reflective microscope objective (RMO); 3-3D adaptor; 4-micro-lens; 5-fiber cable; 6-UV-VIS spectrometer and 7-computer.

barrier filters isolate lights with wavelengths less than 280 nm and 380 nm, respectively.

The system integrated the functions of the aimed OGI location, internal or external sources excitation, weak fluorescence collection, detection and real-time taking photos together. A program to calculate the CIE chromaticity coordinates of the single OGIs by the VIS spectra was also established to precede the color analysis.

Result and Discussion

Homogenization temperature (T_h) and salinity (S)

Microthermometric measurements were conducted on doubly polished thin sections using a heating-freezing stage. The stage was calibrated by use of international standards, providing standard errors on temperature measurements of ± 0.2°C.

Figure 3 shows the homogenization temperature-salinity diagram of the saline inclusions grown in the two episodes in K_2y_{2+3}(a), K_2y_1 (b) and K_2q_{n2} (c) strata of Bai 95 oil well. There are two episodes OGIs in these samples. The first episode grew in the earlier stage of quartz overgrowth. The second episode developed in the later stage of the quartz overgrowth. For the first episode saline inclusions, the average T_h values of the three strata are 75.3, 74.6, and 72.3°C, respectively. And for the second episode saline inclusions, the average values of T_h in the three strata increase to 113.3, 95.4, and 98.7°C, respectively. The increasing amplitudes of the T_hs are 38.0, 20.8 and 23.1°C respectively. For the first episode saline inclusions, the salinities are 7-9%, 6-15% and 9-13% for the K_2y_{2+3}, K_2y_1 and K_2q_{n2} strata respectively. The different *S* values of the saline inclusions in the three strata indicate that in the earlier stage of quartz overgrowth, the original ore-forming fluids have different salinities. In the second episode, the salinities of the saline inclusions in the three strata decrease to 2%, 1.5-5% and 4.5-6%. Compared to the first episode saline inclusions, the average salinities of the second episode saline inclusions decrease 5.9-7.0%. The changes of T_h and S of the saline inclusions indicate that the deposition environment has great change in the later stage of quartz overgrowth. Compared with the earlier stage of quartz overgrowth, the T_h of the strata increase and the S of the ore-forming fluids decrease, which indicate the second episode might be in a water expanding time.

Grains containing oil-gas inclusions (GOIs)

The values of GOIs are different in the two episode stages. In the first episode, the GOIs of the three strata belong to middle value (2-4 ±) [10]. In the second episode, the GOIs of K_2y_1, and K_2q_{n2} strata decrease to 2 ±. But for K_2y_{2+3} stratum, the GOIs increase to 5-6 ±, which shows lots of oil charged K_2y_{2+3} stratum in the second episode.

Polarized fluorescence microscope identification of OGIs

Under the fluorescence microscope, the OGIs of the first episode are liquid phase and very small. They often densely distribute along a line or a stripe. Their colors are often deep brown or grayish brown. The fluorescence intensities are very weak. It is very difficult to measure the fluorescence of such kind of oil inclusions. Figure 4a and Figure 4b shows the microphotos of OGIs grown in the first episode in K_2y_{2+3} stratum (depth: 420.1 m) of Bai 95 oil well. The OGIs formed in the second episode are liquid or liquid-gas phases (Figure 4c and 4d). In a mineral grain, they distributes in group (Figure 4c) or in scattering (Figure 4d). The liquids in the OGIs are colorless, light yellow, light brownish yellow and brown. Under UV light excitation, they generally emit blue or yellowish white fluorescence. Figure 4c and Figure 4d are the OGIs developed in the second episode at 420.1 m in K_2y_{2+3} stratum of Bai 95 oil well. Figure 4e and Figure 4f are the fluorescence image of Figure 4c and Figure 4d when excited by UV light. The OGIs emit strong light yellowish white fluorescence.

Figure 5 shows polarized (a, c, e, g, i and k) and corresponding fluorescence (b, d, f, h, j and l) microphotos of OGIs in the detrital of feldspar (a, c, e, and g), quartz (i) and calcite (k) of K_2y_1 strata in Bai 95 oil well. These OGIs show gas and liquid phase (a, c, e, i and k) and indicate colorless or grey (a), light yellowish grey (c, g and i) and light grey (e). Under excitation at UV light, the OGIs emit strong light bluish green fluorescence (b), strong light yellow fluorescence (d, j and l), strong light yellowish green fluorescence (f), and strong light yellowish white fluorescence (h).

Figure 6 shows the microphotos of OGIs in detrital quartz (a, b and c) and feldspar grains (d, e, f, g, h and i) when excited by monochromatic polarized (a, b, d, f and h) and UV light (c, e, g and i), in K_2q_{n2} stratum (494.6 m), Bai 95 oil well. In which, c, e, g and i are the corresponding fluorescence microphotos of b, d, f, and h. Under excited at UV light, the OGIs emit light yellowish white fluorescence (c), strong light blue and bluish white fluorescence (e), strong light yellow fluorescence (g), and dark brown fluorescence (i).

Combining GOIs with polarized fluorescence microscope

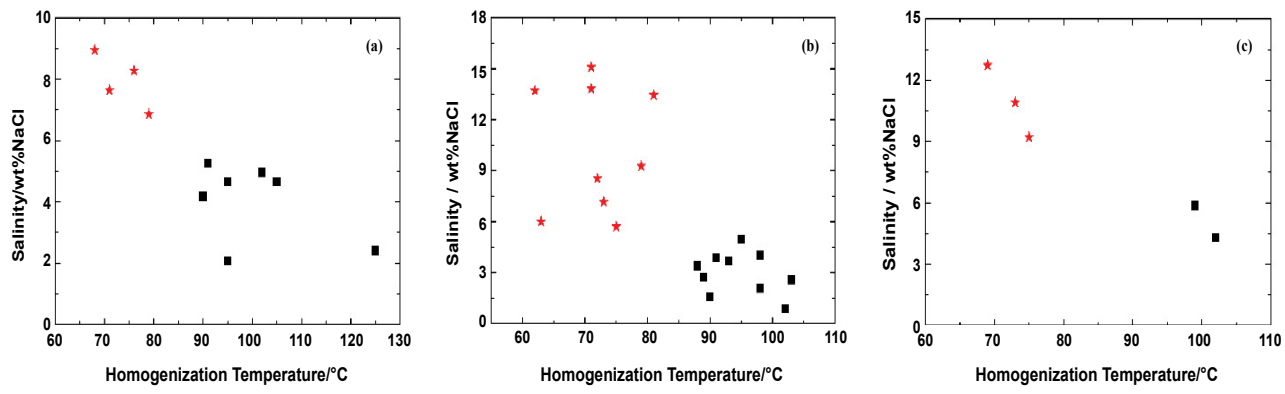

Figure 3: Homogenization temperature-salinity diagrams of the saline inclusions in K_2y_{2+3} (a), K_2y_1 (b) and K_2qn_2 (c) strata in Bai 95 oil well. The star and the square are the first and second episodes inclusions, respectively.

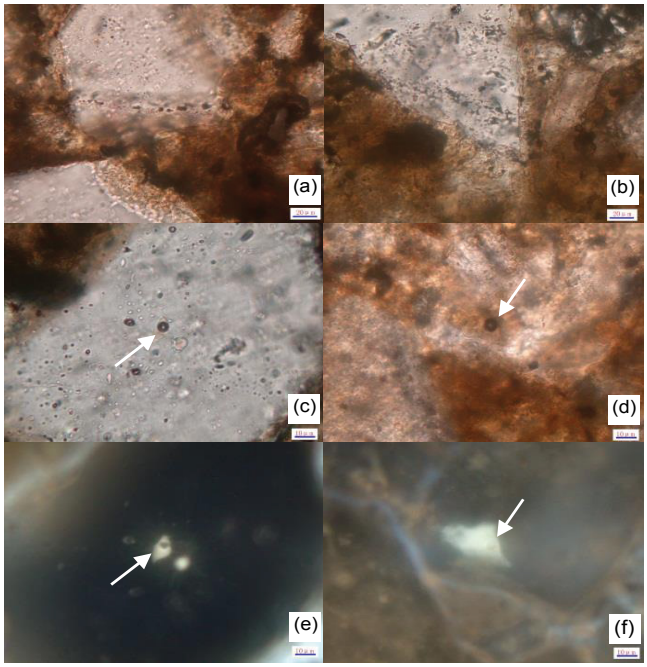

Figure 4: Microphotos of OGIs in K_2y_{2+3} stratum (depth: 420.1 m) of Bai 95 oil well when the OGIs were illuminated by monochromatic polarized (a, b, c, and d) and UV light (e and f). In which, e and f are the corresponding fluorescence microphotos of c and d respectively.

identification of OGIs, oil and gas charging, maturities of palaeo-oils and gases, and the features of maternal source rocks can be estimated. In the earlier stage of quartz overgrowth, a small amount of oil and gas charged K_2qn_2 and K_2y_{2+3} strata. The maturity of the palaeo oil is low. And a certain amount of oil and gas charged K_2y_1 stratum. The maturity of the palaeo oil is low, but the maternal source contains rich organic contents. In the later stage of quartz overgrowth, lots of oil and gas charged K_2q_{n2} and K_2y_{2+3} strata. The multiplier colors of OGIs indicate the oil is heavy and medium hydrocarbons, which may come from two different maternal sources. One is mature source with rich organic matter contents and has good hydrocarbon generation potential; the other is low mature source. This estimate coincides with the analysis of Liu B. Z. et al. [61]. Their research showed that there are two sets of source rocks in Qingshankou and Nengjiang Formations. Liang et al. [59] analyzed the features of heavy oil and its source rocks in the west slope region of Jilin oil field. Their results showed all heavy oils are mature and were mainly generated from source rocks in deep Qingshankou formation in Changling Depression and were not relative to the source rocks in Nenjiang formation. Compared with K_2q_{n2} and K_2y_{2+3} strata, only a certain amount of oil and gas charged K_2y_1 stratum in the second episode. The multiplier colors of the OGIs also indicate not only one maternal source existing or the oil and gas were heterogeneously trapped.

UV-VIS micro-spectroscopy of single OGIs and color analysis

To decreasing the influence from environment, the experiment was conducted in the dark. The main measurement steps are as same

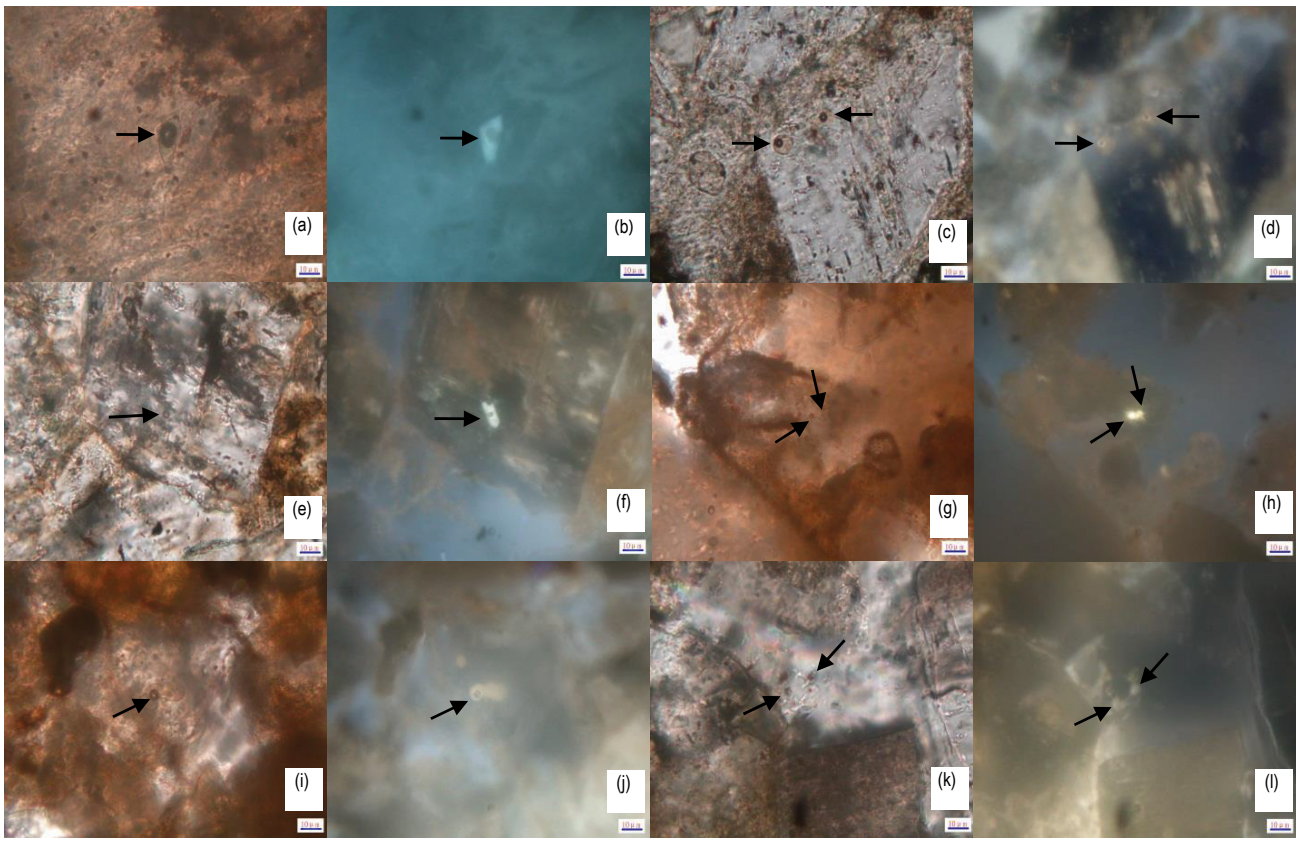

Figure 5: Microphotos of OGIs in the detrital of feldspar (a and b: 426.8 m, c and d: 431.0 m, e and f: 431.0 m, and g and h: 434.5m), quartz (i and j: 431.0 m) and calcite (k and l: 426.8 m) of K_2y_1 stratum in Bai 95 oil well as illuminated by monochromic polarized light (a, c, e, g, i and k) and corresponding fluorescence microphotos under excited at UV light (b, d, f, h, j and l)..

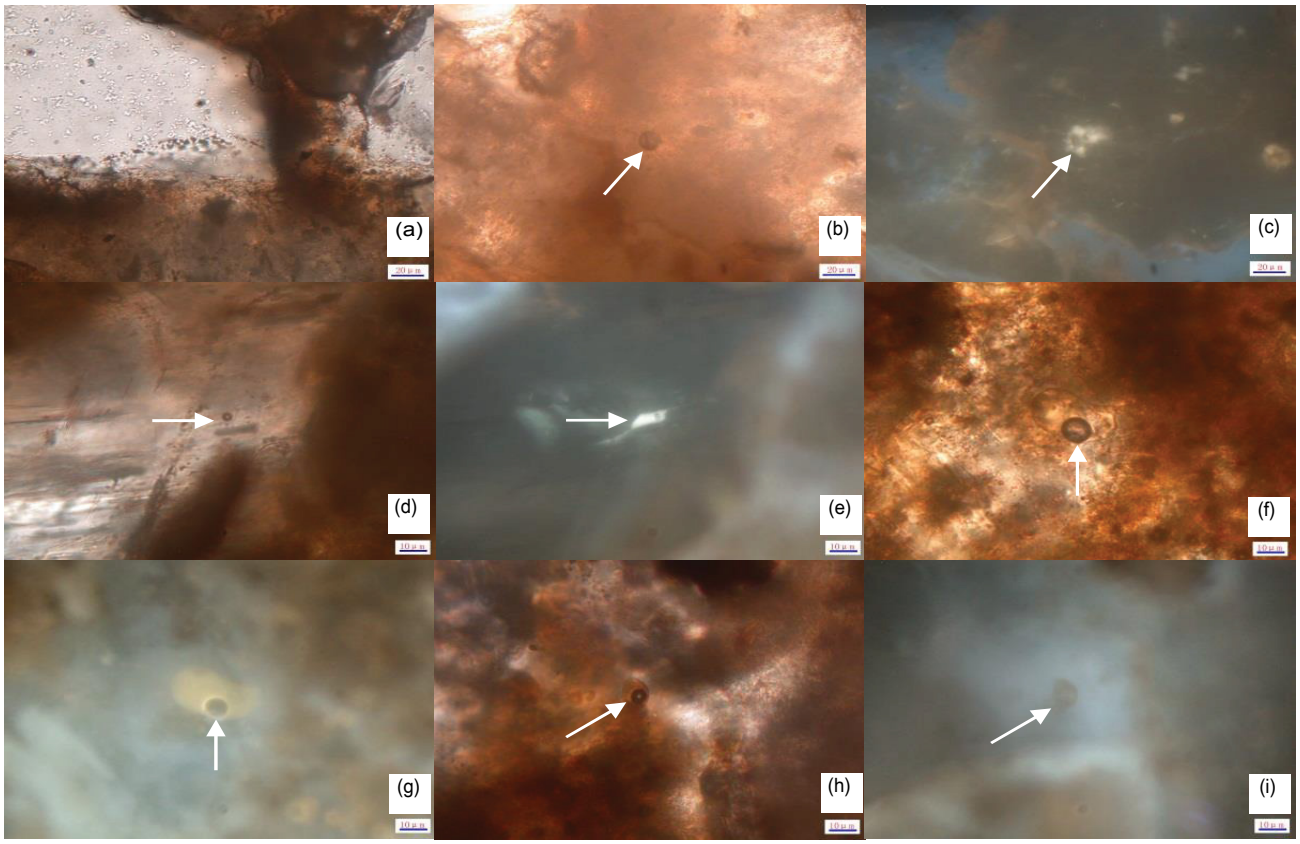

Figure 6: Microphotos of OGIs in detrital quartz (a, b and c) and feldspars grains (d, e, f, g, h and i) when excited by monochromatic polarized (a, b, d, f and h) and UV lights (c, e, g and i), in K_2qn_2 stratum, 494.6 m, Bai 95 oil well. In which, c, e, g and i are the corresponding fluorescence microphotos of b, d, f, and h.

as references [49-51]. A minimum focal spot with size of 12 μm was obtained in our experiment (Figure 7). The halo light around the focal spot is the result of diffraction. It is difficult to be eliminated for the RMO. The focal spot includes most incident energy (84%).

Although the focal spot of the incident light is small, when the size of OGI is less than that of the focal spot, not only the OGI emits fluorescence, but also the background. The background fluorescence is complex. It may origins as following: (1) The mineral grain may contain a few even lots of OGIs unidentified under the IMF [24,62]. (2) The surface of the mineral grain was contaminated by oils existing in the sandstone as preparing the inclusion thin slide. (3) The mineral grain may contain some thulium, which will emit fluorescence when they were excited by light. (4) The inclusion thin slide may be contaminated by organism from air or by observer's hands. So the fluorescence spectrum from the background should be subtracted. For decreasing the influence from the background, a subtract factor should be determined. Because the focal spot includes most excitation energy and its area is small, the energy distribution was approximated to be homogeneous in the spot. The OGI and background were seen as surface light source. Assuming the areas of the OGI and the light spot are S_1 and S_2. The two areas were easily obtained from the microphotos of the OGI (Figure 8a) and the background (Figure 8b). Assuming the luminous intensities from unit surfaces of the OGI and the background are I_i and I_b. And the total fluorescence intensity of the OGI and partial background (S_2-S_1) is $I_1(\lambda)$, the intensity of the background is $I_2(\lambda)$. Then from Eq. (1) and (2), the fluorescence intensity of the OGI is given by

$$I_1 = S_1 I_i + (S_2 - S_1)\, I_b \quad (1)$$

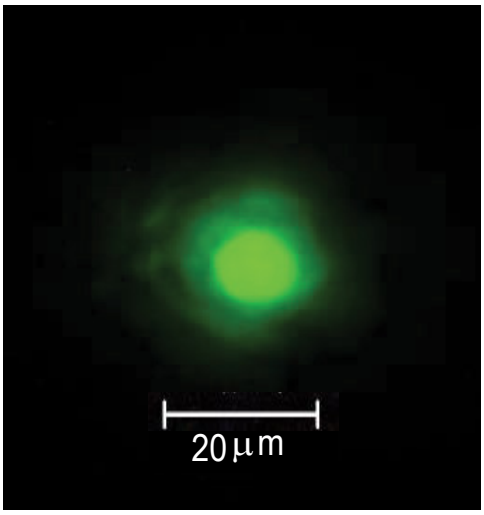

Figure 7: Microphoto of the focal spot with minimum size after external light was guided into the microscope.

$$I_2 = S_2 I_b \quad (2)$$

$$I_i S_1 = I_1 - (1 - \frac{S_1}{S_2}) I_2 = I_1 - F_2 \quad (3)$$

$$F = 1 - \frac{S_1}{S_2} \quad (4)$$

Here F is the subtract factor, which can be obtained from the

microphotos of the OGI (Figure 8a) and the background (Figure 8b). According to Eq. (3) and (4), one can obtain the fluorescence spectra of the single OGI. Following results based on above analysis.

Figure 9 typically shows the transmission (a, e, f, g and h) and reflective (b, c and d) microphotos of an OGI (depth: 494.6 m) in Bai 95 oil well. In which, Figure 9a is the transmission microphoto excited by white light. The inclusion was formed in the second episode and appears liquid and gas phases. Under excited at UV, blue and green internal light sources of the microscope, it showed light yellow (b), strong yellow (c) and influenced by the background. Figure 10a shows the VIS spectra of five different OGIs localized in the three different strata in Bai 95 oil well when excited by the internal UV light source (center wavelength 365 nm). Although the OGIs are different, their spectra look like each other for the interference from the background. And the CIE color coordinates of the single OGIs are also similar (Figure 11a).

When above OGIs were excited by the monochromatic light from the external light source (xeon lamp in the spectrometer), the focal spot size was small, the cement around the OGI was nearly not illuminated, so the fluorescence spectra of the single OGIs were not interfered by the spectra of cements. The background spectra were also subtracted. Figure 10b shows the VIS spectra of the single OGIs as same as Figure 10a excited by the external light source with 365 nm wavelength. One can see that the peak positions of the spectra in Figure 10b are almost as same as Figure 10a. The spectrum of OGI localized at 494.6 m is similar to each other. The other four spectra are different in two aspects. One is the FWHMs are wider as excited by external light source than that of the internal light source. Another is there are "bulks" in the range of 425-610 nm when excited by external light source (Figure 10b), which shows these OGIs contain medium and heavy aromatic hydrocarbons. Above results show that the VIS fluorescence spectra from single OGIs take more information than that of traditional VIS fluorescence spectra without subtracting the interference from background.

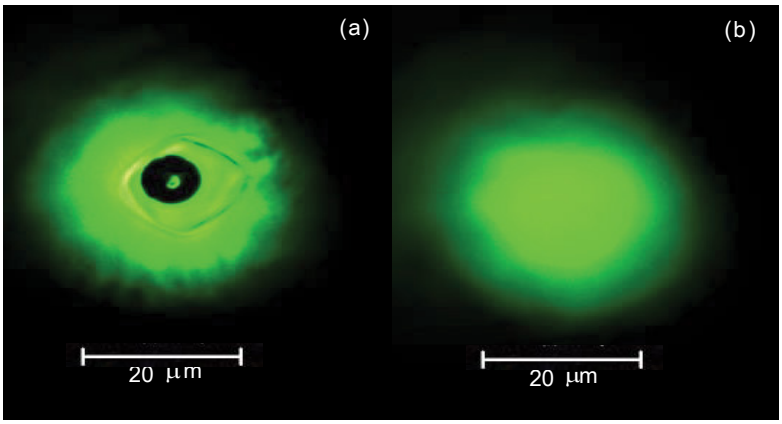

Figure 8: Transmission microphotos of single OGI (a) and the background (b) under excited at external light source with 550 nm wavelength.

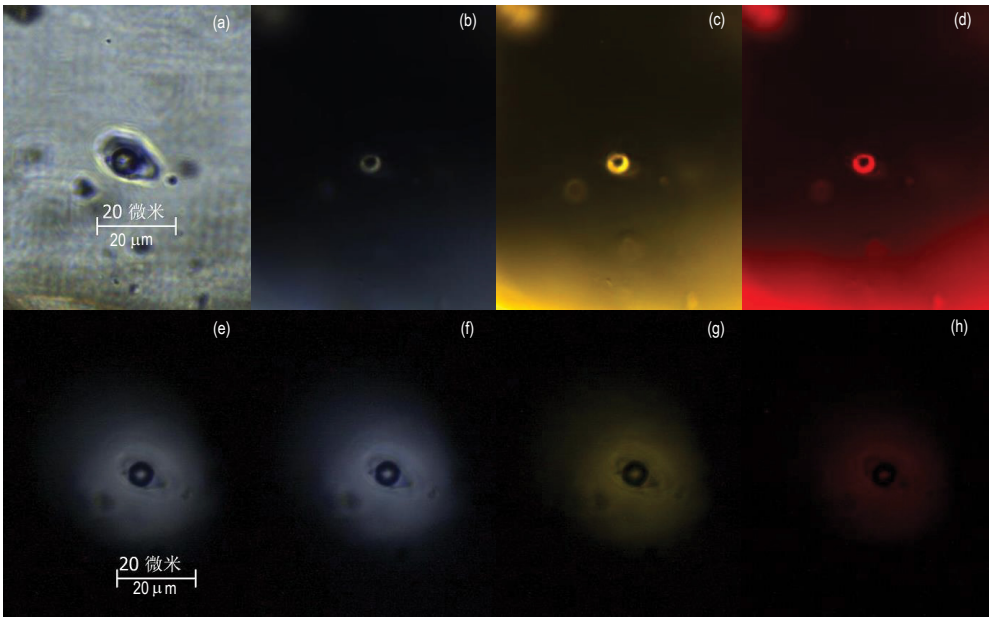

Figure 9: The transmission (a, e, f, g and h) and reflective (b, c and d) micro photos of an OGI (Bai 95, 494.6 m) when white light (a), internal light source (violet(b), blue(c) and green(d)) and external source (250 nm (e), 365 nm (f), 440 nm (g), and 546 nm(h)) were used to excite the single OGI. The scales are all 20 μm.

According to the theory of calorimetric [63], the CIE chromaticity coordinates of OGIs were calculated. Figure 11 shows the CIE chromaticity coordinates of these OGIs excited by internal UV light source (Figure 11a) and external light source (365 nm, Figure 11b). The chromaticity coordinates are in the range of light yellowish white and light bluish white respectively. Compared with the internal UV light excitation, the chromaticity coordinates are more dispersive for single OGIs when excited by external light source. The main reason is that when excited by internal UV light source, not only the single OGI emitting fluorescence, but also other OGIs, the cements and the mineral grain itself, which interfered the fluorescence spectrum of the single OGI, thus the chromaticity coordinates localize in light yellowish white area (Figure 11a). When the external light source was used to excite the single OGI, the light spot was small, the cements and other OGIs were not excited and did not influence the spectrum of the single OGI. The fluorescence of the mineral grain around the under studied OGI has been subtracted as the background. The final spectrum is near to the real spectrum of the under studied OGI, so the chromaticity coordinates are relative dispersive. Above results show that the colors of single OGIs are precise and objective for the spectra are not influenced by the background and observers.

Except for medium and heavy aromatic hydrocarbons, the OGIs may also trap light aromatic hydrocarbons, which emit fluorescence in the range of UV under excited by DUV light, that is to say the fluorescence of these light aromatic hydrocarbons cannot be excited by 365 nm light source. So 250 nm monochromatic light from the external light source was used to excite these OGIs. Figure 12 indicates the UV-VIS spectra of single OGIs from Bai 95 Oil well. The peak positions of the OGI localized at 419.3 m are at 385, 444 and 455 nm. The main aromatic hydrocarbons trapped in the OGIs at K_2y_{2+3} stratum are two, three or four cyclic hydrocarbons. With the buried depth increasing, the fluorescence peaks have red shifts, which indicate that the aromatic hydrocarbons tend to become heavy. The main aromatic hydrocarbons in the OGIs are three, and four cyclic hydrocarbons in the OGIs at K_2y_1 and K_2q_{n2} strata. The peaks near to 545 nm and 610 nm show that there are some heavy aromatic hydrocarbons in these OGIs. The UV-VIS spectra show that there may be two maternal sources charging the strata in the second episode, one is mature, the other is low mature. This result coincides with the analysis of T_h and S. So the main aromatic hydrocarbons and the maturities of palaeo-oils and gases and the features of the maternal sources can be estimated by UV-VIS micro-spectroscopy of single OGIs.

Conclusion

Combining T_h, S, GOIs and polarized fluorescence microscope identification of OGIs together, oil and gas charging, maturities of palaeo-oils and gases, and the features of maternal source rocks related to the three strata of Bai 95 oil well were estimated. In the earlier stage of quartz overgrowth, a small oil and gas charged K_2q_{n2} and K_2y_{2+3} strata,

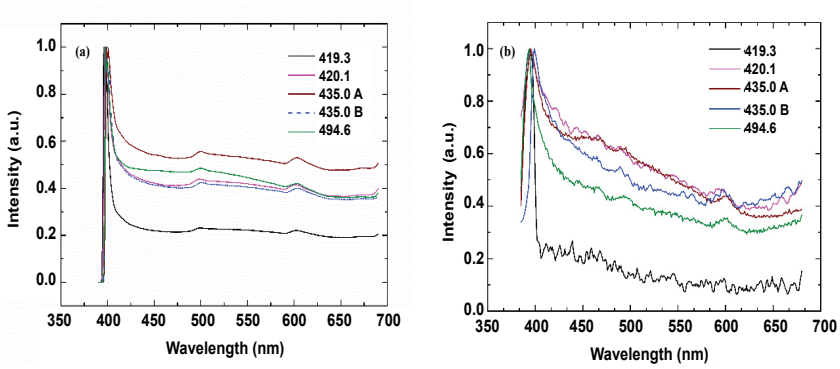

Figure 10: VIS fluorescence spectra of OGIs localized in different depths in Bai 95 oil well when excited by internal UV light source (a, 365 nm) and external light source (b, 365 nm).

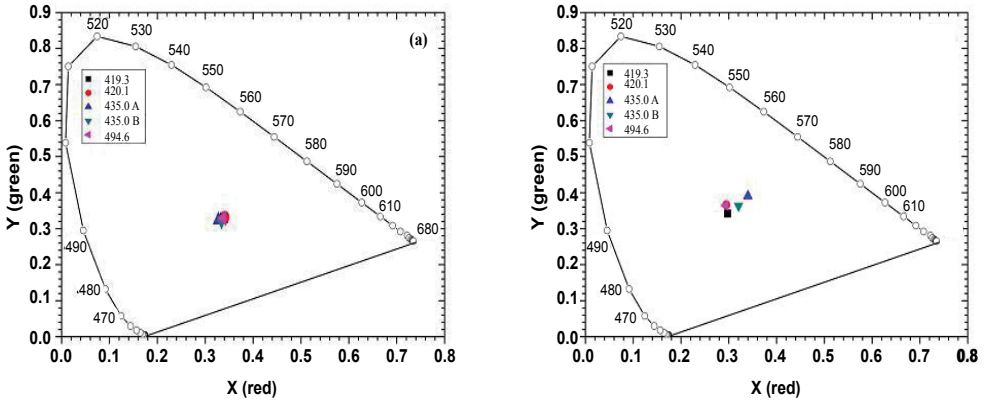

Figure 11: The CIE chromaticity coordinates of OGIs in the Bai 95 oil well when excited by internal UV (a) and external light sources (365 nm, b).

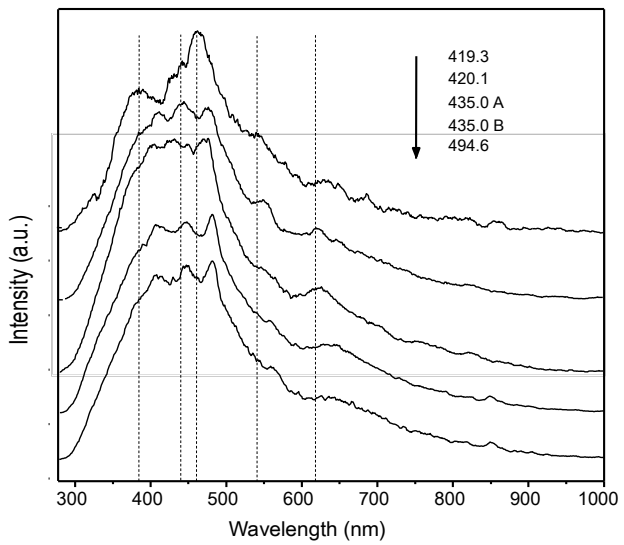

Figure 12: UV-VIS micro-fluorescence spectra of single OGIs formed in the second episode of Bai 95 oil well under excited by external light source with 250 nm wavelength.

and certain amount of oil and gas charged K_2y_1 stratum. The maturity of the palaeo oil is low. In the later stage of quartz overgrowth, lots of oil and gas charged K_2q_{n2}, and K_2y_{2+3} strata, and a certain amount of oil and gas charged K_2y_1 stratum. The multiplier colors of OGIs show the oils are heavy and medium hydrocarbons, which might come from two or more different maternal sources. One is mature source with rich organic matter contents and has good hydrocarbon generation potential; the other is low mature source.

The VIS and UV-VIS spectra of single OGIs were measured under excited by external monochromatic light source. The fluorescence from background was subtracted, so the fluorescence interference from background was greatly decreased. The VIS fluorescence spectra from single OGIs take more information than that of traditional VIS fluorescence spectra without subtracting the interference from background. The CIE chromaticity coordinates of the singles OGIs by the VIS spectra were calculated. The CIE chromaticity coordinates are more objective than those judging by eyes. By analysis the UV-VIS spectra of single OGIs from Bai 95 well, the main aromatic hydrocarbons in the OGIs can be qualitative determined. With the buried depth increasing, the fluorescence peaks have red shifts; the aromatic hydrocarbons tend to become heavy. The UV-VIS spectra showed that there may be two maternal sources charging the strata in the second episode, one is mature, the other is low mature. This result coincides with the analysis results from T_h, S, polarized fluorescence microscope identification of OGIs and GOIs.

In principle, this technique is not limited or limited slightly by the background fluorescence. It can be used to measure the UV-VIS fluorescence of single OGIs trapped in any detrital grains or cements. The fluorescence from light, medium or heavy aromatic contents are all showed on the UV-VIS spectra. Compared with the traditional VIS spectra technique, the fluorescence range is wider. By analysis the UV-VIS spectra, the main aromatic constitutes, the maturities of palaeo-oils and gases, and the oil and gas charging information could be qualitatively estimated. For using a cheap common inversed microscope, but not an expensive DUV microscope, the setup cost was greatly decreased. Our experimental results showed it is a reliable and promising technique in measuring the UV-VIS fluorescence spectra of micro samples, such as bio-inclusions, oils trapped in micro fractures in mineral slides, special mineral grains and so on.

Acknowledgement

This work was supported by the National Nature Science Foundation of China (granted No. 41172110 and 41402108). The author is appreciated for Jilin Oil Field to supply sandstones. The authors deeply thank the reviewers and editors for their constructive suggestions about this manuscript.

References

1. George SC, Lisk M, Summons RE, Quezada RA (1998) Constraining the oil charge history of the South Pepper oilfield from the analysis of oil-bearing fluid inclusions. Org Geochem 29: 631-648.
2. Goldstein RH (2003) Petrographic analysis of fluid inclusions. Fluid inclusions: analysis and interpretation. Mineralogical Association of Canada, short course 32: 9-53.
3. Munz IA (2001) Petroleum inclusions in sedimentary basins: systematics, analytical methods and applications. Lithos 55: 195-212.
4. Dutkiewicz A, Volk H, Ridley J, George SC (2004) Geochemistry of oil in fluid inclusions in a middle Proterozoic igneous intrusion: implications for the source of hydrocarbons in crystalline rocks. Org Geochem 35: 937-957.
5. Blamey NJ, Ryder AG (2009) Hydrocarbon fluid inclusion fluorescence: A Review. Rev Fluor 2007: 299-334.
6. McLimans RK (1987) The application of fluid inclusions to migration of oil and diagenesis in petroleum reservoirs. Appli Geochem 2: 585-603.
7. Bodnar RJ (1990) Petroleum migration in the Miocene Monterey Formation, California, USA: constraints from fluid-inclusion studies. Minera Mag 54: 295-304.
8. Musgrave JA, Carey RG, Janecky DR, Tait CD (1994) Adaption of synchronously scanned luminescence spectroscopy to organic-rich fluid inclusion microanalysis. Rev Sci Instrum 65: 1877-1882.
9. Kirkwood D, Savard MM, Chi G (2001) Microstructural analysis and geochemical vein characterization of the Salinic event and Acadian Orogeny: evaluation of the hydrocarbon reservoir potential in eastern Gaspé. Bull Can Petrol Geo 49: 262-281.
10. Liu KY, Eadington P (2005) Quantitative fluorescence techniques for detecting residual oils and reconstructing hydrocarbon charge history. Org Geochem 36: 1023-1036.
11. Caja MA, Permanyer A, Munz IA, Johansen H (2007) Preliminary data on oil and aqueous fluid inclusions of the fracture-fill in the Corones and Armancies Fms, Eocene, SE Pyrenees. Geogaceta 101: 127-130.
12. Caja MA, Permanyer A, Kihle J, Munz IA, Johansen H (2009) Fluorescence quantification of oil fluid inclusions and oil shows: Implications for oil migration (Armancies Fm, South-eastern Pyrenees, Spain). J Geochem Explor 101: 16.
13. Suchý V, Dobeš P, Sýkorová I, Machovič V, Stejskal M, et al. (2010) Oil-bearing inclusions in vein quartz and calcite and, bitumens in veins: Testament to multiple phases of hydrocarbon migration in the Barrandian basin (lower Palaeozoic), Czech Republic. Mar Petrol Geol 27: 285-297.
14. Bourdet J, Eadington P, Volk H, George SC, Pironon J, et al. (2012) Chemical changes of fluid inclusion oil trapped during the evolution of an oil reservoir: Jabiru-1A case study (Timor Sea, Australia). Mar Petrol Geol 36: 118-139.
15. Burruss RC (1991) Practical aspects of fluorescence microscopy of petroleum fluid inclusions. Luminescence microscopy and spectroscopy: Qualitative and quantitative applications. SEPM Short Course Notes 25: 1-8.
16. Blanchet A, Pagel M, Walgenwitz F, Lopez A (2003) Microspectrofluorimetric and microthermometric evidence for variability in hydrocarbon fluid inclusions in quartz overgrowths: implications for inclusion trapping in the Alwyn North field, North Sea. Org Geochem 34: 1477-1490.
17. Alderton DHM, Oxtoby N, Brice H, Grassineau N, Bevins RE (2004) The link between fluids and rank variation in the South Wales Coalfield: evidence from fluid inclusions and stable isotopes. Geofluids 4: 221-236.
18. Schubert F, Diamond LW, Tóth TM (2007) Fluid-inclusion evidence of petroleum migration through a buried metamorphic dome in the Pannonian Basin, Hungary. Chem Geol 244: 357-381.

19. Bourdet J, Burruss RC, Chou IM, Kempton R, Liu K, et al. (2014) Evidence for a palaeo-oil column and alteration of residual oil in a gas-condensate field: Integrated oil inclusion and experimental results. Geochim Cosmochim Ac 142: 362-385.

20. Xiao XM, Wilkins RWT, Liu ZF, Fu JM (1998) A preliminary investigation of the optical properties of asphaltene and their application to source rock evaluation. Org Geochem 28: 669-676.

21. Xiao XM, Wilkins RWT, Liu DH, Liu ZF, Fu J M (2000) Investigation of thermal maturity of lower Palaeozoic hydrocarbon source rocks by means of vitrinite-like maceral reflectance-a Tarim Basin case study. Org Geochem 31: 1041-1052.

22. George SC, Ruble TE, Dutkiewicz A, Eadington PJ (2001) Assessing the maturity of oil trapped in fluid inclusions using molecular geochemistry data and visually-determined fluorescence colors. Appli Geochem 16: 451-473.

23. Oxtoby NH (2002) Comments on: assessing the maturity of oil trapped in fluid inclusions using molecular geochemistry data and visually-determined fluorescence colours. Appli Geochem 17: 1371-1374.

24. Stasiuk LD, Snowdon LR (1997) Fluorescence micro-spectrometry of synthetic and natural hydrocarbon fluid inclusions: crude oil chemistry, density and application to petroleum migration. Appli Geochem 12: 229-241.

25. Chi G, Lavoie D, Bertrand R (2000) Regional-scale variation of characteristics of hydrocarbon fluid inclusions and thermal conditions along the Paleozoic Laurentian continental margin in eastern Quebec. Can Bull Can Petrol Geol 48: 193-211.

26. Wilkins RW, Wilmshurst JR, Russell NJ, Hladky G, Ellacott MV, et al. (1992) Fluorescence alteration and the suppression of vitrinite reflectance. Org Geochem 18: 629-640.

27. Wilkins RW, Wilmshurst JR, Hladky G, Ellacott MV, Buckingham CP (1995) Should fluorescence alteration replace vitrinite reflectance as a major tool for thermal maturity determination in oil exploration?. Org Geochem 22: 191-209.

28. Lo HB, Wilkins RWT, Ellacott MV, Buckingham CP (1997) Assessing the maturity of coals and other rocks from North America using the fluorescence alteration of multiple macerals (FAMM) technique. Int J Coal Geol 33: 61-71.

29. Veld H, Wilkins RWT, Xiao XM, Buckingham CP (1997) A fluorescence alteration of multiple macerals (FAMM) study of Netherlands coals with “normal” and “deviating” vitrinite reflectance. Org Geochem 26: 247-255.

30. Xiao X, Wilkins RWT, Liu D, Liu Z, Shen J (2002) Laser-induced fluorescence microscopy-application to possible high rank and carbonate source rocks. Int J Coal Geol 51: 129-141.

31. Damaskinos S, Dixon AE, Ellis KA, Diehl-Jones WL (1995) Imaging biological specimens with the confocal scanning laser microscope/macroscope. Micron 26: 493-502.

32. Braeckmans K, Peeters L, Sanders NN, De Smedt SC, Demeester J (2003) Three-dimensional fluorescence recovery after photobleaching with the confocal scanning laser microscope. Biophys J 85: 2240-2252.

33. Sharonov S, Nabiev I, Chourpa I, Feofanov A, Valisa P, et al. (1994) Confocal three-dimensional scanning laser Raman–SERS–fluorescence microprobe. Spectral imaging and high-resolution applications. J Raman Spectrosc 25: 699-707.

34. Schopf JW, Kudryavtsev AB (2009) Confocal laser scanning microscopy and Raman imagery of ancient microscopic fossils. Precambrian Res 173: 39-49.

35. Frezzotti ML, Tecce F, Casagli A (2012) Raman spectroscopy for fluid inclusion analysis. J Geochem Explor 112: 1-20.

36. Pironon J, Canals M, Dubessy J, Walgenwitz F, Laplace-Builhe C (1998) Volumetric reconstruction of individual oil inclusions by confocal scanning laser microscopy. Eur J Mineral 10: 1143-1150.

37. Thiery R, Pironon J, Walgenwitz F, Montel F (2000) PIT (Petroleum Inclusion Thermodynamic): a new modeling tool for the characterization of hydrocarbon fluid inclusions from volumetric and microthermometric measurements. J Geochem Explor 69: 701-704.

38. Zhu G, Zhang S, Liu K, Yang H, Zhang B, et al. (2013) A well-preserved 250 exploration in old and deep basins. Mar Petrol Geol 43: 478-488.

39. Aplin AC, Macleod G, Larter SR, Pedersen KS, Sorensen H, et al. (1999) Combined use of confocal laser scanning microscopy and PVT simulation for estimating the composition and physical properties of petroleum in fluid inclusions. Mar Petrol Geol 16: 97-110.

40. Aplin AC, Larter SR, Bigge MA, Macleod G, Swarbrick RE, et al. (2000) PVTX history of the North Sea's Judy oilfield. J Geochem Explor 69: 641-644.

41. Thiéry R, Pironon J, Walgenwitz F, Montel F (2002) Individual characterization of petroleum fluid inclusions (composition and P–T trapping conditions) by microthermometry and confocal laser scanning microscopy: inferences from applied thermodynamics of oils. Mar Petrol Geol 19: 847-859.

42. Thiéry R (2006) Thermodynamic modelling of aqueous CH_4-bearing fluid inclusions trapped in hydrocarbon-rich environments. Chemical Geol 227: 154-164.

43. Teinturier S, Pironon J, Walgenwitz F (2002) Fluid inclusions and PVTX modelling: examples from the Garn Formation in well 6507/2-2, Haltenbanken, Mid-Norway. Mar Petrol Geol 19: 755-765.

44. Liu DH, Xiao XM, Mi JK, Li XQ, Shen JK, et al. (2003) Determination of trapping pressure and temperature of petroleum inclusions using PVT simulation software-a case study of Lower Ordovician carbonates from the Lunnan Low Uplift, Tarim Basin. Mar Petrol Geol 20: 29-43.

45. Stasiuk LD (1999) Confocal laser scanning fluorescence microscopy of Botryococcus alginite from boghead oil shale, Boltysk, Ukraine: selective preservation of various micro-algal components. Org Geochem 30: 1021-1026.

46. Pironon J, Pradier B (1992) Ultraviolet-fluorescence alteration of hydrocarbon fluid inclusions. Org Geochem 18: 501-509.

47. Kihle J (1995) Adaptation of fluorescence excitation-emission micro-spectroscopy for characterization of single hydrocarbon fluid inclusions. Org Geochem 23: 1029-1042.

48. Munz IA, Wangen M, Girard JP, Lacharpagne JC, Johansen H (2004) Pressure–temperature–time–composition (P–T–t–X) constraints of multiple petroleum charges in the Hild field, Norwegian North Sea. Mar Petrol Geol 21: 1043-1060.

49. Yang A, Ren W, Zhang J, Tang M (2009) A micro-spectroscopy system to measure UV-VIS spectra of single hydrocarbon inclusions. Proc. SPIE 7384, International Symposium on Photoelectronic Detection and Imaging 2009: Advances in Imaging Detectors and Applications.

50. Yang AL, Tang MM, Ren WW, Yang Y, Zhang JL (2011) Investigation of the ultraviolet-visible micro-fluorescence-spectra and chromaticity of single oil inclusion. Acta Optica Sinica 31: 0318002.

51. Yang AL (2012) Based on common inverted microscope to measure UV-VIS spectra of single oil-gas inclusions and colour analysis. Advan Chem Eng Intech.

52. Zhao WZ, Zou CN, Feng ZQ, Hu SY, Zhang Y, et al. (2008) Geological features and evaluation techniques of deep-seated volcanic gas reservoirs, Songliao Basin. Petrol Explor Develop 35: 129-142.

53. Zou CN, Xue SH, Zhao WZ, Li M, Wang YC, et al. (2004) Depositional sequences and forming conditions of the cretaceous stratigraphic-lithologic reservoirs in the Quantou-Nenjiang Formations. Petrol Explor Develop 17: 14-16.

54. Yu-min Z (2006) Conditions of hydrocarbon accumulation of deep reservoirs in the north of Shiwu fault depression in the south of Songliao Basin. J Oil Gas Technol 28: 53-56.

55. Zhang Q, Bao Z, Song X, Sun JW (2008) Hierarchical division and origin of single sand bodies in Fuyu oil layer, Fuyu Oilfield. Petrol Explor Develop 35: 157.

56. Chen ZN, Wand XM, Chen S, Shen XY (2008) Structural evolution of Fuyu reservoir in the Chaochang area of Songliao basin. Geosci 4: 512-519.

57. Zhao ZY, Li HG, Wang XG, Miao HB, Mao CL (2004) Pool formation mechanism of medium shallow layer in south Songliao Basin. Petrol Explor Develop 17:17-19.

58. Tang ZX, Miao HB, Li AM, Yu LX (2003) Hydrocarbon migration characteristics of Nenjiang Formation-Member 4 of Quantou Formation in southern Songliao basin. Geosci 17: 87-91.

59. Liang CX, Liu BZ, Sun WJ (2002) Analysis on the features of heavy oil and its source rocks in the west slope region of the southern Songliao basin. Petrol Explor Develop 29: 45-48.

60. Fu XF, Wang PY, Lu YF, Fu G, Yang M et al. (2007) Tectonic features and control of oil-gas accumulation in the west slope of Songliao basin. Chin J Geol 42: 209-222.

61. Liu BZ, Sun WJ, Cheng SJ, Miao HB (2003) The history of petroleum accumulation in the south of the Songliao basin. Geosci 17:87-91.

62. Meng D, Wu X, Fan X, Meng X, Zheng J et al. (2009) Submicron-sized fluid inclusions and distribution of hydrous components in jadeite, quartz

and symplectite-forming minerals from UHP jadeite–quartzite in the Dabie Mountains, China: TEM and FTIR investigation. Appli Geochem 24: 517-526.

63. Xu XR, Su ZM (2004) Luminescence Theory & Luminescence Materials. Chemical Industry, Beijing.